# Hyperfine Interactions and Electron Spin Distribution in Triplet-State Naphthalene

Noboru Hirota, Clyde A. Hutchison Jr., and Patrick Palmer

# Hyperfine Interactions and Electron Spin Distribution in Triplet-State Naphthalene*

Noboru Hirota, Clyde A. Hutchison Jr., and Patrick Palmer†

*Enrico Fermi Institute for Nuclear Studies, and Department of Chemistry, University of Chicago, Chicago, Illinois*

(Received 5 February 1964)

The anisotropic proton hyperfine interaction of the triplet-state electrons of the naphthalene molecule have been measured at the boiling point of $N_2$. The naphthalene molecules were oriented in single crystal solid solutions in durene. The effects of various substitutions of D for H were investigated. The spin density distribution deduced from these experiments was $\rho_\alpha = +0.219$, $\rho_\beta = +0.062$, $\rho_\gamma = -0.063$. These results were compared with the results of theoretical calculations and with experimental results for the naphthalene negative ion.

## 1. INTRODUCTION

VARIOUS workers have observed proton hyperfine structure in the electron magnetic resonance spectra of naphthalene in its lowest triplet state. Hutchison and Mangum[1] reported preliminary hyperfine structure results for naphthalene molecules oriented in a single crystal of durene. Van der Waals and de Groot[2] have observed hyperfine structure for randomly oriented naphthalene molecules in a glass. Hornig and Hyde[3] have also described hyperfine patterns of naphthalene in durene. Vincent and Maki[4] have investigated the hyperfine structure in the magnetic resonance spectra of quinoxaline.

A discussion of the theory of the spin densities of aromatic molecules in triplet states has been given by McLachlan[5] using both the extended Hartree–Fock method and molecular orbital theory with configuration mixing. The results of numerical calculations of the spin densities in the lowest triplet state of naphthalene have been presented by Amos[6] using the extended Hartree–Fock method.

In this paper we present the results of an extended series of experimental observations on oriented naphthalene molecules in their lowest triplet states with various substitutions of D for H. These results permit relatively reliable and precise determinations of the anisotropic hyperfine interactions with the ring protons. From the sizes of these measured anisotropic interactions we may deduce the spin distributions in naphthalene in its lowest triplet state.

## 2. EXPERIMENTAL PROCEDURES

The results given in this paper are derived mainly from measurements on solute naphthalene in single-crystal solid solutions in solvent durene. A few results of measurements on naphthalene in biphenyl are also presented.

All solvent and solute starting materials used in these experiments were prepared by Merck Sharp & Dohme of Canada Limited. In each case the single crystals were grown in our laboratory by the same method as that used by Hutchison and Mangum[1] in which liquid solutions of naphthalene in solvent were lowered through a temperature gradient to form single-crystal solid solutions.



Fig. 1. Designations of axes for naphthalene and durene.
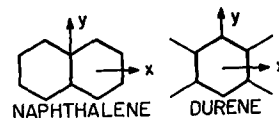
The crystals were mounted and oriented in the microwave resonant cavity as described by Hutchison and Mangum.[1] The monoclinic symmetry axis is in all cases easily located by means of the characteristic cleavage plane patterns. The durene crystals were mounted on wedges as previously described[1] with their $c$ axes parallel to rulings on the surfaces of the wedges. These wedges have been designed on the basis of the x-ray structure determinations to hold the durene crystals in the resonant cavity so that the laboratory magnetic field **H** may be moved in one of the three principal magnetic planes of one of the two durene molecules per unit cell. As shown before, the naphthalene solute molecules are incorporated substitutionally in the durene structure so that their triplet-state fine structure $x$, $y$, and $z$ axes are parallel, respectively, to the $x$, $y$, and $z$ axes of the durene molecules. These axes are shown in Fig. 1. The positions of the two principal axes for any given mounting of the crystal were easily found by rotating the field **H** until the appropriate stationary points were located using oscilloscope patterns as indicators.

In all cases the principal axes of the hyperfine interaction were assumed to coincide with those of the fine structure.

[1] C. A. Hutchison, Jr., and B. W. Mangum, J. Chem. Phys. **34**, 908 (1961).

[2] Reported by P. Kottis and R. Lefebvre, J. Chem. Phys. **39**, 393 (1963).

[3] A. W. Hornig and J. S. Hyde, Mol. Phys. **6**, 33 (1963).

[4] J. S. Vincent and A. H. Maki, J. Chem. Phys. **39**, 3088 (1963).

[5] A. D. McLachlan, Mol. Phys. **5**, 51 (1962).

[6] A. T. Amos, Mol. Phys. **5**, 91 (1962).

TABLE I. Hyperfine structure. Naphthalene-2,3,6,7-$d_4$ in perdeuterodurene.

| 1 | 2 | 3 | 4 | 5 | 6 | 7 |
|---|---|---|---|---|---|---|
| Axis | Series number | Number of curves | Hyperfine structure splittings best values $\bar{\delta}$ (gauss) | $\sigma\{\bar{\delta}\}$ (gauss) | Linewidth, best values $\bar{w}$ (gauss) | $\sigma\{\bar{w}\}$ (gauss) |
| $x$ | 1 | 3 | 7.83 | 0.07 | 2.33 | 0.06 |
|  | 2 | 2 | 7.62 | 0.09 | ... | ... |
|  | 3 | 2 | 7.73 | 0.08 | 2.19 | 0.04 |
|  | | Series best value | 7.73 | 0.07 | | |
| $z$ | 1 | 4 | 5.57 | 0.04 | 1.91 | 0.05 |
|  | 2 | 4 | 5.67 | 0.05 | 1.88 | 0.04 |
|  | 3 | 4 | 5.59 | 0.07 | 2.08 | 0.04 |
|  | | Series best value | 5.61 | 0.04 | | |
| $y$ | 1 | 7 | 2.48 Gaussian fit | 0.10 | 6.78 | 0.06 |
|  | 2 | 3 | | | 6.86 | 0.14 |
|  | | | | Average | 6.82 | 0.11 |

Most of the measurements were made using pen recordings on charts, subsequent to the initial orienting along principal axes. The magnetic field axis on the recordings was calibrated in separate runs in which markers were placed on the charts at various field strengths with values determined by proton resonance. Magnetic field strengths were measured in the same manner as described by Hutchison and Mangum.[1]

The measurements were made at frequencies in the near vicinity of $9.535 \times 10^9$ sec$^{-1}$ and at fields between $3.6 \times 10^3$ and $4.5 \times 10^3$ G. A total of six different crystals of naphthalene in durene and one crystal of naphthalene in biphenyl were used for these experiments. The concentrations of the naphthalene were not measured for the crystals used in this work but ultraviolet absorption spectrum measurements on crystals prepared under similar conditions have shown mole fractions of naphthalene in durene in the range of $1 \times 10^{-3}$ to $4 \times 10^{-3}$.

The $x$-axis hyperfine structures were observed during experiments in which **H** was rotated in the $xz$ plane of one molecule; $y$-axis structures were observed during rotations in the $yz$ plane; $z$-axis structures were observed during rotations in the $xz$ plane.

All of the quantitative results reported here were obtained with the resonant cavity immersed in boiling $N_2$ and under continuous illumination of the crystal with an A-H6 high-pressure mercury arc. The temperatures of the crystals have been found to be approximately 10°K higher than the cryostat bath temperature in experiments in which thermocouples were placed in the crystals during illumination.

## 3. EXPERIMENTAL RESULTS

### 3.1. Naphthalene in Durene

#### 3.1.1. Naphthalene-2,3,6,7-$d_4$

The experimental results for naphthalene-2,3,6,7-$d_4$ in perdeuterodurene are summarized in Table I. Typical recorder curves are shown in Figs. 2, 3, and 4 for **H**
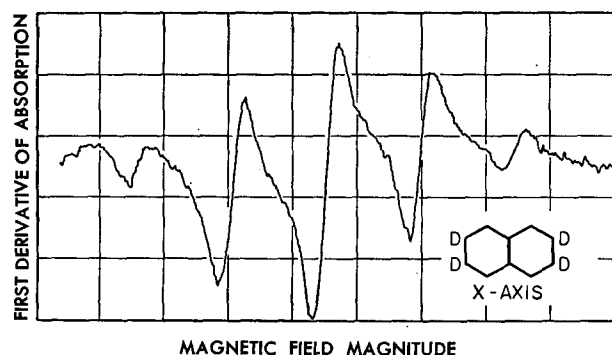


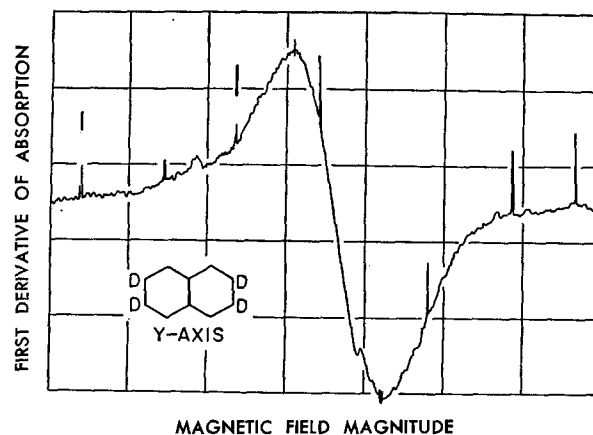FIG. 2. Naphthalene-2,3,6,7-$d_4$ hyperfine pattern with **H** || $x$ axis.



FIG. 3. Naphthalene-2,3,6,7-$d_4$ hyperfine pattern with **H** || $y$ axis.

TABLE II. Hyperfine structure. Naphthalene-2-$d_1$ in perdeuterodurene, H $\parallel$ z axis.

| 1 | 2 | 3 | 4 | 5 | 6 |
|---|---|---|---|---|---|
| Peak number | Chart No. 1 peak positions (gauss) | Chart No. 2 peak positions (gauss) | Average peak positions (gauss) | Oscilloscope peak positions (gauss) | Best calculated peak positions (gauss) |
| 1–1′ | 0.65 | 0.65 | 0.65 | 0.63 | 0.64 |
| 2–2′ | 1.99 | 1.97 | 1.98 | 1.92 | 2.01 |
| 3–3′ | 3.58 | 3.52 | 3.55 | 3.58 | 3.55 |
| 4–4′ | 4.89 | 4.83 | 4.86 | 5.03 | 4.93 |
| 5–5′ | 6.19 | 6.11 | 6.15 | 6.32 | 6.20 |
| 6–6′ | 7.48 | 7.40 | 7.44 | 7.53 | 7.53 |
| 7–7′ | 8.90 | 8.94 | 8.92 | 8.90 | 8.94 |
| 8–8′ | 10.27 | 10.23 | 10.25 | 10.44 | 10.36 |
| 9–9′ | 11.97 | 11.73 | 11.85 | 11.87 | 11.86 |
| 10–10′ | 13.18 | 12.92 | 13.05 | 13.11 | 13.11 |

along the $x$, $y$, and $z$ axes, respectively. Each series of measurements was made on one crystal only. All the measurements of a given series were made without disturbing the mounting of the one single crystal used in the series. Different crystals were used in different series but all the different crystals of naphthalene-2,3,6,7-$d_4$ came from the same single-crystal growth. Of the various recorder curves used in these measurements there was always at least one scan with increasing $|\mathbf{H}|$ and at least one with decreasing $|\mathbf{H}|$ on the same crystal and the same axis. For each of the five-peak curves for the $x$ axis and for the $z$ axis, the value of the nearest-neighbor peak-to-peak separation, which gave a least squares fit to all five peaks, was calculated. It was assumed that all four intervals should theoretically be equal. This best value of the separation is the $\bar{\delta}$ entered in Column 4 of the table. The standard deviation of $\bar{\delta}$ is the $\sigma\{\bar{\delta}\}$ entered in Column 5. Application of the $t$ test[7] shows that the differences between the values of



FIG. 4. Naphthalene-2,3,6,7-$d_4$ hyperfine pattern with H $\parallel$ z axis.

[7] N. Arley and K. R. Buch, *Introduction to the Theory of Probability and Statistics* (John Wiley & Sons, Inc., New York, 1950), p. 170.

$\bar{\delta}$ for the various series are not quite large enough to give clear indication that the different mountings of the crystals corresponded to different true values for the peak intervals because, for example, of different orientations leading to different hyperfine spacings. Therefore all the peaks of all the series for a single axis were least-squares fitted by the same single-peak separation $\delta$ labeled series best value in Table I.

The linewidths listed in Table I are distances between maxima and minima in the derivatives of the absorptions.

As seen from Fig. 3, the $y$-axis pattern did not contain resolved peaks. Therefore the experimental curves were compared with a series of curves, each synthesized by the superposition of five Gaussians equally spaced and with intensities in the ratios 1:4:6:4:1. Throughout the series of superpositions the value of $\Delta/a$ was varied, where $\Delta$ is the width of a Gaussian and $a$ is the interval between two Gaussians. The value of $\Delta/a$ which most nearly simulated both the shape and width at maximum slope $\gamma$ of the experimental curves was found to be 0.80. The experimental curves show just a very slight trace of structure. Values of $\Delta/a$ just slightly larger than 0.80 completely removed the structure and gave distinctly worse fits to the data. The value of $\gamma/a$ for the best fit was 2.75. It was found that $\gamma/a$ was very insensitive to variation of $\Delta/a$. The values, 0.90, 0.80, 0.70, for $\Delta/a$ yielded, respectively, the values 2.81, 2.75, 2.71 for $\gamma/a$. The separation given in Column 4 of Table I is 1/2.75 times the experimentally observed width of the $y$-axis peak, and from the considerations mentioned above it will be seen that this separation is known quite reliably.

### 3.1.2. Naphthalene-2-$d_1$

The experimental results for naphthalene-2-$d_1$ with H along the $z$ axis are summarized in Table II. The experimental 10-peak pattern from one of the charts is shown in Fig. 5. The numbers in Column 1 are the labels of a peak–valley pair, assumed theoretically equi-
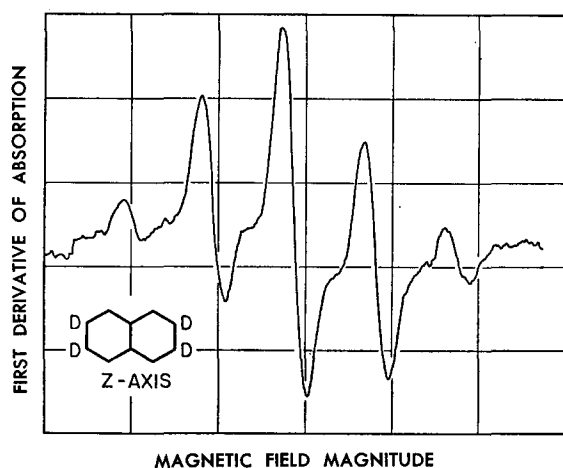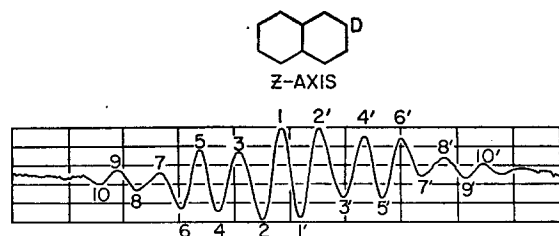
FIG. 5. Naphthalene-2-$d_1$ hyperfine pattern with **H** $\|$ $z$ axis.

distant from the center of the pattern. The peaks and valleys are given the designations shown in Fig. 5. The numbers entered in Column 2 and Column 3 are $\frac{1}{2}$ the peak–valley separations as measured on the calibrated chart. The average of the two charts which were run are given in Column 4 and similar determinations using an oscilloscope trace are shown in Column 5.

### 3.1.3. *Other Systems*

The experimental results for other systems are given in Table III, together with three recorder curves which were run for naphthalene-2-$d_1$ with **H** parallel to the $x$ axis. The resulting twelve nearest-neighbor peak intervals of the three resolved five-peak spectra for naphthalene-2-$d_1$ were averaged to give $\bar{\delta}$ and the standard deviation is given in the table. The data for naphthalene-1-$d_1$ were obtained from the resulting four-peak oscilloscope pattern and for naphthalene-1,4-$d_2$ from the three-peak recorder curve.

### 3.2. Naphthalene in Diphenyl

For naphthalene in diphenyl five recorder curves were run with **H** along the $y$ axis. These showed well-resolved five-peak patterns. The distances from the centers of the patterns to first peaks on the right and to first peaks on the left were measured for each curve. These 10 distances were averaged yielding the value 2.46 G. The 10 distances from the first peaks on the right to the second peaks on the right and from the first peaks on the left to the second peaks on the left were averaged yielding the value 2.50 G.

### 4. DISCUSSION OF RESULTS

#### 4.1. General Remarks

The isotropic component of the proton hyperfine interactions with the $\pi$-electron systems of aromatic free radicals (i.e., doublet-state molecules) is now well understood due to the extensive investigations which have followed the original theoretical and experimental work of McConnell,[8] Bersohn,[9] Weissman,[10] and

Jarrett.[11] This isotropic interaction which requires a finite electron spin density at the in-plane proton arises from the interaction between the $\sigma$ electrons of the C–H bond and the $\pi$ electrons and is closely proportional to the spin density on the C adjacent to the proton.

In a few cases the anisotropic hyperfine interaction between a proton and a $\pi$ electron on an adjacent C atom due to the direct dipole–dipole force has been observed. This interaction is also quite accurately proportional to the electron spin density on the adjacent C atom in those systems which have been previously investigated. This anisotropic dipole–dipole interaction has, however, not been observed in aromatic ring systems because the paramagnetic species (positive and negative ions) are normally available only in liquid solutions where the tumbling motions of the molecules annihilate the anisotropic components of the hyperfine splittings. It has however been studied in such systems as the malonic acid radical $CH(COOH)_2$,[12] irradiated amino acids,[13,14] and triphenylmethyl.[15]

In the case of the electron magnetic resonances of triplet-state naphthalene molecules oriented in host crystals we have an ideal opportunity for investigating both the isotropic and anisotropic components of the interaction in an aromatic molecule between the triplet $\pi$-electron system and the ring protons.

### 4.2. Assumptions

In discussing the experimental triplet-state hyperfine structures described in the previous sections of this

TABLE III. Hyperfine structure.

| 1<br>System | 2<br>Axis | 3<br>Number of curves | 4<br>Hyperfine structure splitting, $\delta$ (gauss) | 5<br>$\sigma\{\bar{\delta}\}$ (gauss) |
|---|---|---|---|---|
| Naphthalene-2-$d_1$<br>in perdeuterodurene | $x$ | 3 | 7.74 | 0.04 |
| Naphthalene-1-$d_1$<br>in perdeuterodurene | $x$ | 1 | 8.03 | ... |
| Naphthalene-1,4-$d_2$<br>in perdeuterodurene | $x$ | 1 | 8.08 | ... |
| Naphthalene<br>in diphenyl | $y$ | 5 | 2.46 | 0.08 |
|  |  |  | 2.50 | 0.11 |
| Average | ... | — | 2.48 | ... |

[11] H. S. Jarrett, J. Chem. Phys. **25**, 1289 (1956).
[12] T. Cole, C. Heller, and H. M. McConnell, Proc. Natl. Acad. Sci. (U.S.) **45**, 525 (1959); H. M. McConnell, C. Heller, T. Cole, and R. W. Fessenden, J. Am. Chem. Soc. **82**, 766 (1960).
[13] D. K. Ghosh and D. H. Whiffen, Mol. Phys. **2**, 285 (1959).
[14] I. Miyagawa and W. Gordy, J. Chem. Phys. **30**, 1590 (1959).
[15] F. C. Adam and S. I. Weissman, J. Am. Chem. Soc. **80**, 2057 (1958).

[8] H. M. McConnell, J. Chem. Phys. **24**, 764 (1956).
[9] S. I. Weissman, J. Chem. Phys. **25**, 890 (1956).
[10] R. Bersohn, J. Chem. Phys. **24**, 1066 (1956).

paper we approximate the existing situation with a model based on the following assumptions.

(1) The isotropic part $a$ of the hyperfine interaction arises only from separate interactions within the eight individual C–H fragments, four of them in equivalent $\alpha$ positions and four in equivalent $\beta$ positions in the ring. The contribution to the isotropic interaction with the proton adjacent to the $i$th C atom is proportional to the spin density in the $p_c$ orbital on the $i$th C atom.

(2) The contribution of the spin density in the $p_z$ orbital on the $i$th C atom to the anisotropic dipole–dipole interaction with the proton adjacent to the $i$th atom is the same, per unit spin density, as in the case of the central C–H fragment of the malonic acid radical investigated experimentally by Cole, Heller, and McConnell.[12]

(3) The contribution of the $p_z$ orbital on the $i$th C atom to the dipole–dipole interaction with the adjacent proton is proportional to the spin density in that $p_z$ orbital.

(4) The proportionality constants for the interaction described in Sec. 4 are the same for both the $\alpha$ and $\beta$ positions.

(5) The contribution of the spin density $\rho_j$, in the $p_z$ orbital on the $j$th C atom to the interaction with the proton on the $i$th C atom, $i \neq j$, is equal to that of two spin densities, each of size $\frac{1}{2}\rho_j$, located at points equal distances above and below (with respect to the aromatic plane) the $j$th C atom. These distances are taken to be the most probable distances from the C atom for an electron in a Slater C orbital.

(6) The naphthalene molecule possesses orthorhombic symmetry. The $\alpha$ C–H bonds are all parallel to the $y$ axis of the molecule. The $\beta$ C–H bonds all make angles of magnitude $2\pi/6$ with the $x$ axis of the molecule. All C–H bonds have the same length. The two rings are regular hexagons. (The actual structure has been determined by Robertson.[16])

## 4.3. Numerical Values

The numerical values of the various quantities used in applying this model to the discussion of the experimental results are assumed to be those given below.

(1) The proportionality constant $Q$, between the spin density $\rho$ in the $p_z$ orbital of a C–H fragment and the isotropic part $a$ of the hyperfine interaction energy in the relation $a = Q\rho$, is given by $Q/h = -63.08 \times 10^6$ sec$^{-1}$ per unit spin density. This value results from Tuttle and Weissman's[17] measured hyperfine splitting, 3.75 G, for the benzene negative ion, the isotropic $g$ value given below, and the use of $\rho = \frac{1}{6}$ for each C–H fragment of the benzene negative ion. The effects of the size of the molecular electric charge on the value of $Q$ are neglected.

(For a discussion of the effect of molecular electric charge on $Q$ in the case of doublet species the work of Colpa and Bolton[18] should be consulted.)

(2) The spin density in the $p_z$ orbital on the central C atom of the malonic acid radical is 0.892. This value is taken from Karplus and Fraenkel[19] who compute it from the measured proton hyperfine interaction and their value, $Q_{CH}{}^H = -23.72$ G, for the CHC$_2$ fragment. The experimental values of Cole, Heller, and McConnell and of McConnell, Heller, Cole, and Fessenden[12] for the proton hyperfine interaction energies, $A$, $B$, and $C$ (isotropic part plus dipole–dipole part) in the malonic acid radical, namely, $A/h = -30.0 \times 10^6$ sec$^{-1}$ [along the C–H axis ($A$ axis)], $B/h = -61.5 \times 10^6$ sec$^{-1}$ [along the axis of the $p_z$ orbital ($B$ axis)], and $C/h = -92.5 \times 10^6$ sec$^{-1}$ [along the third mutually perpendicular axis ($C$ axis)] then give the values, $A_d/h = +35.1 \times 10^6$, $B_d/h = -0.2 \times 10^6$, and $C_d/h = -35.0 \times 10^6$ sec$^{-1}$ for the dipole–dipole interaction energies, $A_d$, $B_d$, and $C_d$ along the $A$, $B$, and $C$ axes, respectively, per unit spin density.

(3) The $p_z$ orbitals are Slater orbitals,

$$\phi_\pi = (K^3/32\pi)^{\frac{1}{2}} Re^{-R/2} \sin\theta \cos\phi,$$

with $K \equiv Z/a_0$, $Z = 3.18$, $a_0 = 0.529 \times 10^{-8}$ cm, $R = Kr$. The most probable distance from the C atom for an electron in this orbital is $0.83 \times 10^{-8}$ cm.

(4) The lengths of all C–H bonds are $1.08 \times 10^{-8}$ cm. The lengths of all C–C bonds are $1.40 \times 10^{-8}$ cm.

(5) The fine structure is described by the spin Hamiltonian, $\mathcal{H} = |\beta| \mathbf{H} \cdot g \cdot \mathbf{S} + \mathbf{S} \cdot T \cdot \mathbf{S}$, in which $S = 1$; $g$ is isotropic and has the value $+2.0030$; and the principal values of $T/hc$ are $T_{zz} \equiv D = +0.1012$ cm$^{-1}$ $T_{xx} = T_{yy} \equiv E = -0.0141$ cm$^{-1}$.

## 4.4. Calculations

We have calculated the spin density distribution using from our data only those given in Tables I and II. (The model given in Sec. 4.2 and the numerical values given in Sec. 4.3 were of course used.) We have assumed that the measured hyperfine interactions are negative.

For the measurements summarized in Table I for naphthalene-2,3,6,7-$d_4$ we were observing the hyperfine interactions from the 4 $\alpha$ protons only. When **H** was parallel to the $x$, $y$, or $z$ axes of the naphthalene molecule **H** was also at the same time parallel to the $C$, $A$, or $B$ axes, respectively, of the four C–H fragments. [See 4.3(2) for the definitions of the $A$, $B$, $C$ axes.] The splittings measured in this case therefore give directly the three splittings along the $A$, $B$, and $C$ axes of the $\alpha$ C–H fragments.

It is to be noted that in the present case (contrary to the malonic acid radical case) the $A$, $B$, and $C$ axes are not precisely along the canonical directions[12] of the total isotropic plus anisotropic hyperfine interaction

[16] J. M. Robertson, Proc. Roy. Soc. (London) **A141**, 594 (1933); **A142**, 659 (1933).
[17] T. R. Tuttle and S. I. Weissman, J. Am. Chem. Soc. **80**, 5342 (1958).
[18] J. P. Colpa and J. R. Bolton, Mol. Phys. **6**, 273 (1963).
[19] M. Karplus and G. K. Fraenkel, J. Chem. Phys. **35**, 1312 (1961).

TABLE IV. Hyperfine interaction energies $\times h^{-1}$.

| 1 | 2 | 3 | 4 |
|---|---|---|---|
| Measured splitting (gauss) | $\left(\dfrac{\text{Hyperfine interaction energy}}{h}\right)$[a] (sec$^{-1}$) | $\left(\dfrac{\text{Dipole–dipole part of hyper-fine interaction energy}}{h}\right)$[b] (sec$^{-1}$) | $\left(\dfrac{\text{Isotropic part of hyperfine interaction energy}}{h}\right)$[b] (sec$^{-1}$) |
| $\lvert \delta_{\alpha x}\rvert = 7.73\pm0.07$ | $C_\alpha/h = -(21.41\pm0.20)\times10^6$ | $C_{d\alpha}/h = -(6.75\pm0.17)\times10^6$ | |
| $\lvert \delta_{\alpha y}\rvert = 2.48\pm0.10$ | $A_\alpha/h = -(6.77\pm0.27)\times10^6$ | $A_{d\alpha}/h = +(7.89\pm0.20)\times10^6$ | $a_\alpha/h = -(14.66\pm0.12)\times10^6$ |
| $\lvert \delta_{\alpha z}\rvert = 5.61\pm0.04$ | $B_\alpha/h = -(15.81\pm0.11)\times10^6$ | $B_{d\alpha}/h = -(1.15\pm0.13)\times10^6$ | |
| $\lvert \delta_{\beta z}\rvert = 2.29\pm0.04$ | $B_\beta/h = -(6.45\pm0.11)\times10^6$ | $\cdots$ | $\cdots$ |

[a] The algebraic signs given in Column 2 are assumed.

[b] The signs in Columns 3 and 4 follow from the signs assumed for Column 2.

tensor of an individual C–H fragment because of the large contributions of $p_z$ orbitals on $C$ atoms outside the fragment to the dipole–dipole component of the interaction. However, these outside contributions lead to canonical directions (along which both the electron spin and the nuclear spin are well quantized and the hyperfine interactions are independent of size of field) which are sufficiently close to the $A$ and $C$ axes, in the case of the $\alpha$ fragment, that the local field deviates from the lab field by only an angle of approximately 0.01 rad. For the $B$ axis, the direction is exactly canonical for both the $\alpha$ and $\beta$ fragments. Hence, the assumptions made in this paper about canonical directions are extremely close to reality.

For the measurements summarized in Table II for naphthalene-2-$d_1$ H was parallel to the $z$ axis of the naphthalene molecule and hence at the same time parallel to the $B$ axes of all seven C–H fragments (both $\alpha$ and $\beta$ fragments). These patterns (see Fig. 5) are therefore the resultants of two fundamental splittings, the one, $\delta_\alpha$, associated with the four $\alpha$ protons and the other, $\delta_\beta$, associated with the three $\beta$ protons. Gaussian syntheses were made for various values of $\delta_\alpha/\delta_\beta$ and for various values of the width at maximum slope $\Delta$. Some of these syntheses are shown in Fig. 6, together with the corresponding values of $\delta_\alpha/\delta_\beta$ and $\Delta$. In all of these syntheses $\lvert\delta_\alpha\rvert$ was taken to be the value of the splitting measured for naphthalene-2,3,6,7-$d_4$ with H parallel to the $z$ axis of the molecule ($B$ axes of the C–H fragments), namely, 5.61 G. It is clear from Fig. 6 and from Table II that the best fit obtained by Gaussian synthesis reproduces very well the general appearance of the experimental curve and gives a good quantitative fit of the peak and valley positions. A comparison of the calculated peak and valley positions given in Column 6 of Table II with the experimental values given in Columns 4 and 5 of Table II shows very good agreement. Figure 6 also shows that the choice of parameters for the synthesis is quite critical and that they are therefore determined quite precisely by the experiments.

We estimate that the standard deviation in $\delta_\alpha/\delta_\beta$ to be approximately 0.05.

The best fit to the experimental curve was obtained with $\delta_\alpha/\delta_\beta = 2.45$ and $\Delta = 1.70$ G. The best value of $\lvert\delta_\beta\rvert$ was therefore $5.61/2.45 = 2.29$ G.

The four experimentally obtained numbers which we now utilize are therefore

$$\lvert\delta_{\alpha x}\rvert = 7.73\pm0.07\text{ G}, \qquad \lvert\delta_{\alpha y}\rvert = 2.48\pm0.10\text{ G},$$

$$\lvert\delta_{\alpha z}\rvert = 5.61\pm0.04\text{ G}, \qquad \lvert\delta_{\beta z}\rvert = 2.29\pm0.04\text{ G}$$

$$= \frac{5.61\pm0.04}{2.45\pm0.05}\text{ G}$$

These values are also listed in Column 1 of Table IV.

It is now necessary to compute from the four experimental splittings the hyperfine interaction energies, $A_\alpha$, $B_\alpha$, $C_\alpha$, and $B_\beta$ along the $A$ axis, $B$ axis, and $C$ axis of the $\alpha$ C–H fragment and the $B$ axis of the $\beta$ fragment, respectively. We must remember that with nonvanishing $E$ in the spin Hamiltonian of 4.3(5) the value of $\partial W/\partial\lvert\mathbf{H}\rvert$ is not independent of $\lvert\mathbf{H}\rvert$, where $W$ is an eigenvalue of the Hamiltonian. There is, hence, no single conversion factor for converting from field strength (gauss) to frequency (reciprocal seconds) or to energy, as in the case of aromatic or other free radicals. We must also remember that the states are not simply the strong-field states $\lvert 1\rangle$, $\lvert 0\rangle$, and $\lvert\bar{1}\rangle$ but for example when $\mathbf{H}$ is parallel to the $z$ axis, are the linear combinations $\cos\theta\,\lvert 1\rangle + \sin\theta\,\lvert\bar{1}\rangle$, $\lvert 0\rangle$, and $\sin\theta\,\lvert 1\rangle - \cos\theta\,\lvert\bar{1}\rangle$, where $\tan 2\theta = E/G$ and $G = g_{zz}\lvert\beta\rvert\,\lvert\mathbf{H}\rvert$. Similar linear combinations must be taken for the other orientations. Inasmuch as we are primarily interested in hyperfine interaction energies for the states $\lvert 1\rangle$, $\lvert 0\rangle$, and $\lvert\bar{1}\rangle$ we must take this fact into account. We of course make the assumptions of Sec. 4.3(5).

In the manner indicated in the immediately preceding paragraph, i.e., by correcting the measured magnetic field splittings for nonlinearity of energy with field and
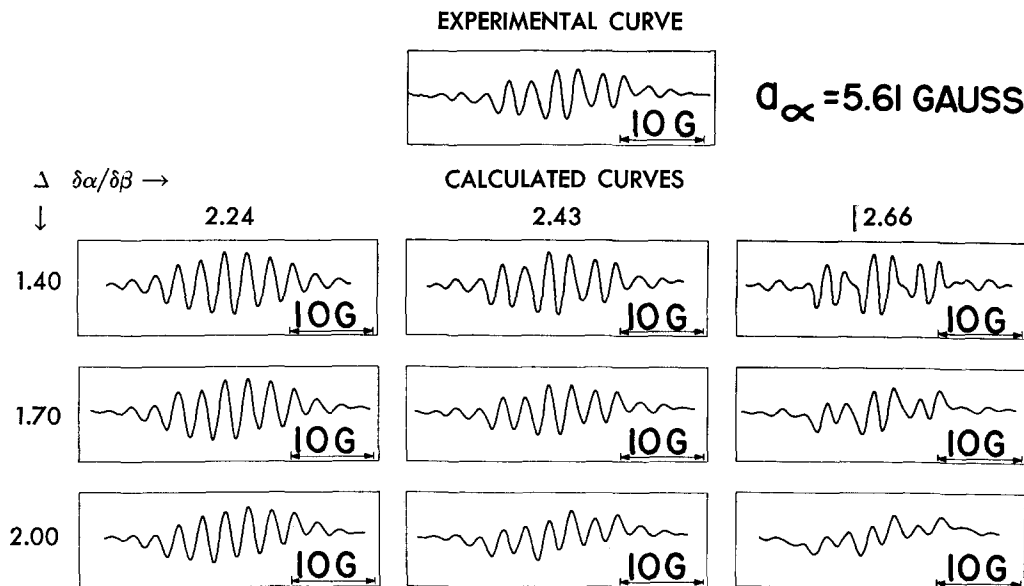
FIG. 6. Gaussian syntheses of hyperfine patterns for naphthalene-2-$d_1$ with H || $z$ axis for various values of $\delta_\alpha/\delta_\beta$ and of $\Delta$.

for state mixing, we arrive at the values listed in Column 2 of Table IV for the hyperfine interaction energies, $A_\alpha$, $B_\alpha$, $C_\alpha$, $B_\beta$ along the $A$ axis, $B$ axis, and $C$ axis of the $\alpha$ C–H fragment and the $B$ axis of the $\beta$ fragment, respectively. These axes are defined in Sec. 4.3(2) and as already noted are not principal axes of the interaction for an individual fragment. The negative algebraic signs given in Column 2 of Table IV are assumed. No signs were determined by the experiments. The three components, $A_{d\alpha}/h$, $B_{d\alpha}/h$, $C_{d\alpha}/h$ of the traceless dipole–dipole anisotropic part of the $\alpha$ hyperfine interaction are listed in Column 3. The isotropic part of the $\alpha$ hyperfine interaction is given in Column 4.

We now must estimate the spin density distribution from the hyperfine interaction energies in Table IV. The procedure which we follow consists of the following steps. The model described in Sec. 4.2 is used.

(1) An arbitrary spin density distribution is assumed.

(2) The contribution from $p_z$ orbitals on all not nearest C atoms to the dipole–dipole interaction, $A_{d\alpha}$, $B_{d\alpha}$, $C_{d\alpha}$, with the $\alpha$ proton is computed.

(3) This contribution is subtracted from the measured dipole–dipole interaction of Column 3, Table IV.

(4) This corrected dipole–dipole interaction is then divided by (1/0.892) times the experimentally determined dipole–dipole interaction[12] in the C–H fragment of the malonic acid radical [see 4.3(2)].

(5) The average of the two numbers obtained in (4) from the corrected $A_{d\alpha}$ and $C_{d\alpha}$ is used as a new $\alpha$ spin density for an iteration of steps (4) through (5). A new $\beta$ spin density is assumed for the iteration such that $\rho_\alpha/\rho_\beta$ is the same as for the initial arbitrary spin density. $\rho_\gamma$ for the central C atoms is taken such that

$$4\rho_\alpha + 4\rho_\beta + 2\rho_\gamma = 1.$$

(6) Iterations are continued until self-consistency is obtained.

(7) The self-consistent spin density distribution (with given fixed $\rho_\alpha/\rho_\beta$) is now used to compute the contribution of spin density in $p_z$ orbitals on not nearest C atoms to the measured ratio, 2.45, of $\alpha$ splitting to $\beta$ splitting when H was along the $z$ axis of the molecule (see above for the derivation of the value 2.45).

(8) This corrected ratio is compared with the fixed spin density ratio $\rho_\alpha/\rho_\beta$ used in the iterations of Steps (1) through (6).

(9) A new spin density ratio $\rho_\alpha/\rho_\beta$ is assumed and the iteration of Steps (1) through (6) is repeated.

(10) The calculation of (7) is then repeated and the comparison of (8) is made.

(11) The steps (9) and (10) are repeated until the corrected ratio, of (7), equals the assumed spin density ratio $\rho_\alpha/\rho_\beta$ used in the iteration of Steps (1) through (5).

The values of the spin densities yielded by the procedure just described are $\rho_\alpha = +0.219$, $\rho_\beta = +0.062$, $\rho_\gamma = -0.063$, $\rho_\alpha/\rho_\beta = 3.52$. Inasmuch as the standard deviation in the $A$ and $C$ dipole–dipole components of the hyperfine interaction (see Table IV) is approximately 2.5% the error in $\rho_\alpha$ arising from our measurements has about this same value. The ratio $\rho_\alpha/\rho_\beta$ is very sensitively determined by the iterative method, and therefore $\rho_\alpha$ is subject to a 2.5% uncertainty. These uncertainties lead to a standard deviation of approximately 8% in $\rho_\gamma$. It is of course difficult to estimate the uncertainties introduced by the use of the numerical values cited in 4.3.

It is to be noted that when H is parallel to the $z$ axis of the naphthalene molecule and therefore parallel to the $B$ axes of all eight C–H fragments the ratio of the

Table V. Spin densities.

| | Results of present work | | | | | | | |
| | From anisotropic part | From isotropic part $Q/h=-63.08\times10^6$ sec⁻¹ See 4.3(1) | From isotropic part $Q/h=-66.50\times10^6$ sec⁻¹ | Calculation by Amos[a] for lowest triplet state | Single Hückel orbital, (5, 5') configuration | Pariser[b] calculation for lowest triplet state | Hoyland and Goodman[c] calculation for lowest triplet state | Experimental value of Atherton and Weissman[d] for negative ion, $Q/h=-63.06\times10^6$ sec⁻¹ |
| | 1 | 2 | 3 | 4 | 5 | 6 | 7 | 8 |
|---|---|---|---|---|---|---|---|---|
| $\rho_\alpha$ | +0.219 | +0.232 | +0.220 | +0.235 | +0.181 | +0.168 | +0.198 | +0.220 |
| $\rho_\beta$ | +0.062 | ... | ... | +0.048 | +0.069 | +0.074 | +0.052 | +0.083 |
| $\rho_\gamma$ | −0.063 | ... | ... | −0.066 | 0.000 | +0.015 | 0.000 | −0.106 |
| $\rho_\alpha/\rho_\beta$ | +3.52 | ... | ... | +4.89 | +2.62 | +2.27 | +3.81 | +2.65 |

[a] See Ref. 6.
[b] See Ref. 22.
[c] L. Goodman and J. R. Hoyland, J. Chem. Phys. 39, 1068 (1963).
[d] N. M. Atherton and S. I. Weissman, J. Am. Chem. Soc. 83, 1330 (1961).

two splittings which yield the experimental patterns is 2.45. The ratio, 3.52, of the computed spin densities is quite different from the ratio of the two splittings. This difference arises, of course, from the dipole–dipole contributions from $p_z$ orbitals on the not nearest C atoms.

We may also estimate the value of the spin density $\rho_\alpha$ by using the value obtained for the isotropic part of the $\alpha$ hyperfine interaction $a_\alpha$ measured for naphthalene-2,3,6,7-$d_4$ and given in Column 4, Table IV. This value is $a_\alpha/h = -14.66\times10^6$ sec⁻¹. We use this value in conjunction with the value $Q/h = -63.08\times10^6$ sec⁻¹ in the relation $\rho_\alpha = a_\alpha/Q$ and obtain $\rho_\alpha = +0.232$. This disagrees with the value estimated from the anisotropic component by only 6%. Use of the value, $Q/h = -66.50\times10^6$ sec⁻¹ (from Karplus and Fraenkel's value[19], $Q_{CH}{}^{H} = -23.72$ G for the CHC₂ fragment; also very closely McLachlan's preferred value [20] for $Q/h$ in aromatic systems) yields $\rho_\alpha = +0.220$ which is very close to the value obtained from the measured anisotropic interaction, namely, +0.219.

### 4.5. Comparisons

It is interesting to compare these spin densities which are estimated from the experimental results for the ground triplet state of naphthalene with theoretical estimates and with the experimental values for the naphthalene negative ion. Experimental values for the naphthalene positive ion are at present unavailable. The various sets of values are given in Table V.

The experimental values for the triplet state are in relatively good agreement with the calculations by Amos[6] who uses the unrestricted Hartree–Fock method. McLachlan[20] had pointed out that Löwdin's[21] projection method could in principle be employed to remedy the undesirable property of the unrestricted wavefunction for computing spin densities, namely, that it is not an eigenfunction of $S^2$, and Amos[6] does this. McLachlan[20] has however shown that in radicals (doublet states) this defect of the unrestricted wavefunction does not invalidate the calculated spin densities and leads to approximately correct values for the relatively large negative spin densities in aromatic molecules. The same large negative values are also given by molecular orbital theory with configuration mixing. By application of the same methods to a discussion of triplet states of aromatic molecules, McLachlan[5] has shown that also in this case the exchange effects on the correlations of the electrons produce large negative spin densities. It is, of course, well known that the negative ion, the positive ion, and the singly excited configuration for the lowest triplet will all give the same spin density distribution because of the pairing theorem. Moreover, McLachlan[5] shows that even when one includes the exchange polarization corrections which yield negative spin densities, this statement is still true and the distribution for the lowest triplet is still the same as for the positive and negative

[20] A. D. McLachlan, Mol. Phys. 3, 233 (1960).
[21] P.-O. Löwdin, Phys. Rev. 97, 1509 (1955).

ions. It is only when the mutual correlations of (a) the excited electron and of (b) the hole which it leaves in the closed shell are taken into account that one gets a new effect which gives some expected differences between the spin distributions for the triplets and for the doublets. MaLachlan[5] has shown that these effects may be expected to be relatively small. There is an additional effect which must be considered and which we have mentioned in a previous paper, namely, the doubly excited configurations such as have been found by Pariser[22] for the lowest triplet state of naphthalene. This effect never leads to any negative spin densities and in the particular case of naphthalene leads to relatively small deviations from the spin densities expected for the single excitation of lowest energy.

The present work indeed bears out the theoretical prediction of MaLachlan[5] that the spin density distribution for the lowest triplet state of naphthalene should closely resemble that of the negative ion. Experimentally the $\alpha$ spin densities are essentially identical in the two cases. The value of $\rho_\alpha/\rho_\beta$ is larger for the triplet molecule than for the negative ion by the factor 1.33. The negative spin density on the central C's is 1.7 times as large for the negative ion as for the triplet. It is difficult to see that the observed small differences between the doublet and triplet states bear any close resemblance to the differences computed by Amos[6] except for the fact that they are relatively small.

The best values obtained, as described above, by the iterative calculation of the spin densities from the experimental hyperfine splittings may be used to obtain the principal values of the dipole–dipole component of the hyperfine interaction of the $\alpha$ proton with the $p_z$ orbital on the adjacent C atom only (subtracting interaction with the $p_z$ orbitals on not nearest C atoms). This gives, per unit spin density,

$$A_{d\alpha}'/h = +34.7 \times 10^6 \text{ sec}^{-1},$$
$$B_{d\alpha}'/h = +0.9 \times 10^6 \text{ sec}^{-1},$$
$$C_{d\alpha}'/h = -35.5 \times 10^6 \text{ sec}^{-1}.$$

[22] R. Pariser, J. Chem. Phys. **24**, 250 (1956).

This iterative calculation of course uses the experimental parameters,[12] namely,

$$A_d/h = +35.1 \times 10^6 \text{ sec}^{-1},$$
$$B_d/h = -0.2 \times 10^6 \text{ sec}^{-1},$$
$$C_d/h = -35.0 \times 10^6 \text{ sec}^{-1}$$

per unit spin density, to yield the spin density at each state of the iteration as described in Sec. 4.4(4).

The isotropic part of the $\alpha$ hyperfine interaction, $-14.66 \times 10^6$ sec$^{-1}$, divided by the $\alpha$ spin density, $+0.219$, obtained in our calculation gives $-66.9 \times 10^6$ sec$^{-1}$ as the isotropic interaction per unit spin. This is quite close to the experimental value[12] for the malonic acid radical which is $-68.7 \times 10^6$ sec$^{-1}$ per unit spin if we take the spin density on the central C to be 0.892. The calculation forces no agreement in the case of this isotropic part.

It is thus seen that our results for the hyperfine interactions of the $\alpha$ proton in naphthalene in its lowest triplet state are in agreement with the assumption that these interactions, both isotropic and anisotropic, are exceedingly close to those of the proton of the central C–H fragment of the malonic acid radical.

Lastly it should be noted that when we use the value of $Q$ found experimentally for the electrically charged naphthalene negative ion [corrected for difference in $g$, see Sec. 4.3(1)] together with our experimental value of the triplet-state isotropic interaction, we get a result for $\rho_\alpha$ which is in very good agreement with that obtained from the experimental value of the anisotropic interaction. This indicates that effects of charge on the $Q$, such as those discussed by Colpa and Bolton[18] are not important in this case.

### ACKNOWLEDGMENTS